Chapter 5

Stable Matching Based Revenue Maximization for Federated Learning in UAV-Assisted WBANs

5.1 Introduction

WBAN usage in healthcare has rapidly grown, with sensors placed on patients to collect physiological data for transmission to an LD [54]. These systems address resource scarcity in hospitals and facilitate remote health monitoring [8]. WBANs also enable the development of effective ML models using the abundant physiological data. Moreover, the growth of 5G network has led to the use of UAVs to address the complex WBAN infrastructure, leveraging their agility, flexibility, and mobility [10]. This growth is also reflected in the Drones-as-a-Service (DaaS) industry, where independent drone owners offer on-demand data collection and model training [10]. UAVs are typically categorized into two types: fixed-wing and rotary-wing UAVs [117]. Fixed-wing UAVs provide high-speed flight capabilities while carrying heavy payloads, whereas rotary-wing UAVs, with limited velocity and payload capacity, are better suited for stationary communication applications [117]. UAVs play a crucial role in supporting resource-constrained WBANs,

especially in outdoor events and remote areas, by collecting physiological data from WBANs and performing model training for applications, such as HAR [11] and disease detection [12, 13].

To enhance the inference model, independent UAV companies can collaborate by sharing collected physiological data from WBANs for model training [10]. However, sharing data from multiple sources to a central server faces challenges due to limited network resources, resulting in data islands. To this end, we propose the adoption of a FL [14] approach to enable privacy-preserving collaborative ML across independently owned UAVs. This approach assists resource-constrained WBANs with data collection and model training, ensuring privacy and communication efficiency through FL.

Typically, a *model owner* initiates an FL task to collect physiological data from WBAN users across different regions via rotary-wing UAVs for model training. Moreover, the model owner *incentivizes WBANs* to contribute their physiological data and UAVs to collect data from WBANs and perform model training. Specifically, *WBANs aim to maximize their revenue by contributing data, while UAVs aim to maximize their revenue through model training within the model owner's maximum budget.* To this end, we advocate using *stable matching* based RA approach in UAV-assisted WBAN-based FL framework where UAVs gather data from WBANs to train an FL model, with the help of a Macro Base Station (MBS) owned by the model owner, as shown in Fig. 5.1. However, this framework faces several challenges due to limited 5G radio resources, i.e., PRBs[1], which affects the QoS in HD as can be seen in Table 5.1 [16, 17]. Moreover, there is a need to prioritize RA strategies based on the criticality of the data. For instance, patients with heart disease require continuous monitoring, where heart rate, blood pressure, and blood sugar level detection take priority over body temperature data. Hence, it is crucial to allocate minimal resources for transmitting critical data while allocating maximum resources to WBANs for transmitting complete data if the

[1]PRB is the smallest unit of radio resource in cellular 5G networks, comprises a 0.5 *ms* time slot and a 180 kHz frequency band [15].

Table 5.1: QoS requirement

Sensor type	Required throughput	Required PRBs
Blood saturation	16 bps	1
Body temperature	120 bps	1
EEG	43.2 kbps	2
ECG	144 kbps	5
Motion sensor	35 kbps	2
Voice	100 kbps	4

required resources are available. However, the growing number of WBANs with varying PRB demands for transmitting physiological data to UAVs may result in interference, presenting a unique challenge in 5G for real-time smart healthcare applications.

Traditional UAV-based FL frameworks [10,50,117] primarily focus on enhancing the inference model, neglecting RA that considers UAVs' revenue, network interference, and critical data transmission, altogether. Existing works [55, 56] address interference through effective channel allocation but aren't directly applicable to our proposed model. On the other hand, work in [48] focuses on improving the inference model through FL utilizing distributed healthcare data. In contrast, this chapter emphasizes on RA by considering interference, revenue, and prioritizing the transmission of critical patient data. Moreover, we formulate an optimization problem that maximizes revenue of WBANs and UAVs via RA, considering resource demands while minimizing interference among WBANs, altogether. Additionally, we propose an efficient sub-optimal solution based on *stable matching* [30,31] and *graph coloring* approaches to solve the formulated revenue maximization problem while considering resource demands of WBANs. The graph coloring approach, in particular, is motivated by the need to efficiently manage interference among WBANs, where two interfering WBANs cannot be allocated the same PRB—a scenario that can be modeled as a graph [118]. To this end, we convert the WBAN topology into an interference graph, $G(\mathbb{V}, \mathbb{E})$ (see Subsection 5.3.1), where nodes represent WBANs and edges denote interference between them, facilitating effective interference management by ensuring that no two adjacent nodes (i.e., inter-

fering WBANs) are assigned the same PRB. This problem is analogous to the graph coloring problem, where adjacent nodes must be assigned different colors. The main contributions of this chapter are summarized as:

- Propose a UAV-assisted WBAN-based FL framework[2] where UAVs gather physiological data from WBANs and perform model training with the help of an MBS, to develop smart healthcare applications.
- Formulate an optimization problem that maximizes the revenue of WBANs and UAVs via RA while considering minimum and maximum resource demand, as well as interference among WBANs in 5G network, as an NP-hard problem.
- Solve the formulated problem efficiently using stable matching and graph coloring-based approaches in polynomial time complexity.
- Simulation and prototype results on real-world data show the efficacy of the proposed model, achieving 92.8% of the optimal value.

5.2 System Model

We consider a healthcare system, where a model owner wishes to collect data from a set of WBANs denoted by $\mathbb{P} = \{1, \ldots, p, \ldots, P\}$ using UAVs presented by $\mathbb{U} = \{1, \ldots, u, \ldots, U\}$ for model training, such as for HAR [11] and disease detection [12], as shown in Fig. 5.1. Let $\mathbb{S} = \{1, \ldots, s, \ldots, S\}$ be the set of sensors in a WBAN to capture physiological data and send it to an LD using either Bluetooth - an IEEE 802.15.1 standard designed for short-range wireless communication with a focus on security and low power consumption, or ZigBee - an IEEE 802.15.4 standard intended for use in sensor and control applications due to its low power consumption[3]. Moreover, we assume that WBANs are equipped with 5G communication capability, and transmission of health data from WBANs to UAVs occurs through a high-speed 5G network. After collecting

[2]This chapter focused on revenue maximization via RA for FL in UAV-assisted WBANs rather than performing actual FL model training; however, we plan to address this aspect in future work.

[3]A detailed explanation for these standards is provided in [38, 119].

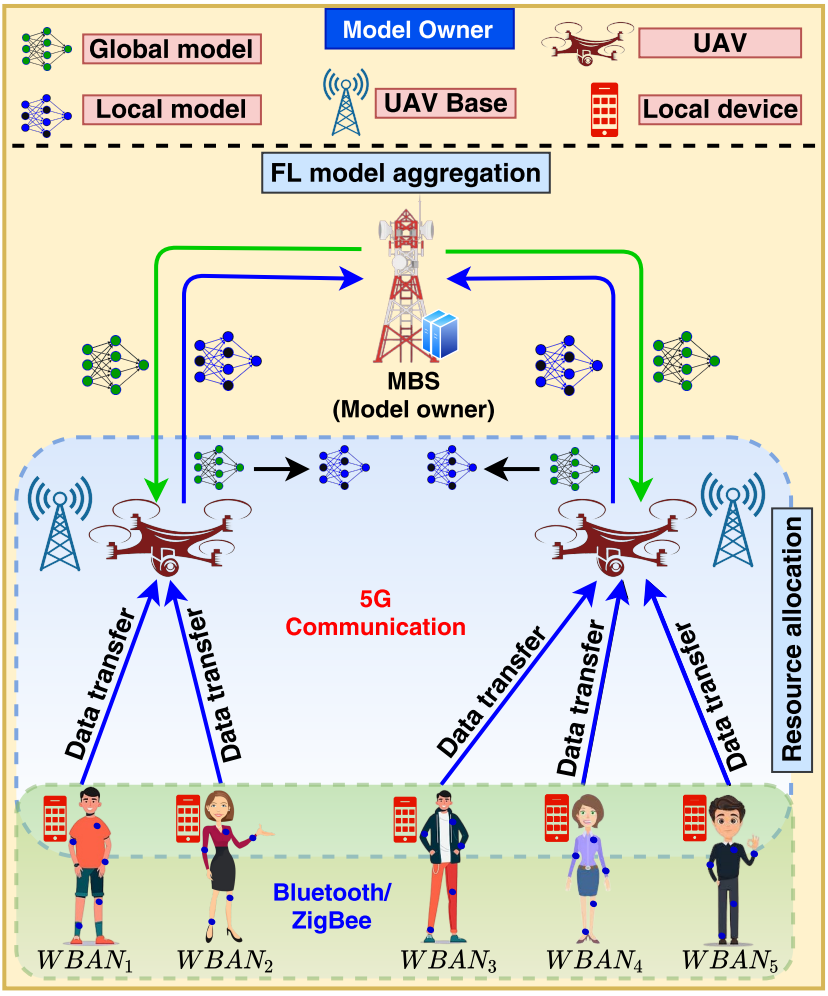

Fig. 5.1. UAV-assisted WBAN-based FL framework.

the data, UAVs return to UAV base for FL model training with the help of MBS[4]. However, any two WBANs may interfere with each other during data transmission to UAV, causing packet collision and data loss [54]. To avoid interference, MBS allocates PRBs to WBANs, considering various parameters, as discussed in the following.

5.2.1 Required PRBs for Data Transmission

Let WBAN p requires a throughput of $\mathfrak{T}_p^s$ to transmit physiological data collected by sensor s to UAV via *Orthogonal Frequency-Division Multiple Access* (OFDMA) technique. Then, the relation between the required number of PRBs $\mathfrak{J}_p^s$ and the throughput

[4]We assume that the connection between UAV base and MBS is via a high-speed LAN cable [120].

$\mathfrak{T}_p^s$ is given as [121]:

$$\mathfrak{J}_p^s = \left\lceil \mathfrak{T}_p^s / (\mathfrak{H}\mathscr{F}) \right\rceil, \tag{5.1}$$

where $\mathscr{F}$ denotes efficiency in bits/symbol of the used modulation and coding scheme and $\mathfrak{H} = (\Im\wp)/\mathrm{T}_{sf}$, depends on network configuration. $\Im$ and $\wp$ represent number of sub-carriers and symbols per PRB, respectively; and T_{sf} is frame duration. Here, $\mathrm{T}_{sf} = 0.5\ ms$, $\wp = 7$ and $\Im = 12$ [121].

To ensure successful physiological data transmission, WBANs have minimum and maximum PRB demands, where the minimum demand ensures the successful transmission of critical data, and the maximum demand guarantees the transmission of all data. The minimum PRB demand ($\mathfrak{J}_p^{min}$) for WBAN p is computed as the sum of required PRBs for transmitting each sensor s's data with a criticality index ρ_p^s (discussed in Eq. (3.2) of Chapter 3) exceeding the threshold value ρ_{th}, while the maximum PRB demand ($\mathfrak{J}_p^{max}$) represents total required PRBs for transmitting all data of WBAN p, as:

$$\begin{cases} \mathfrak{J}_p^{min} = \sum_{s\in\mathbb{S}, \rho_p^s \geq \rho_{th}} \mathfrak{J}_p^s. \\ \mathfrak{J}_p^{max} = \sum_{s\in\mathbb{S}} \mathfrak{J}_p^s. \end{cases} \tag{5.2}$$

For instance, let WBAN p is equipped with blood saturation, body temperature, and EEG sensors, with criticality indices for the health data collected by them being 0.7, 0.6, and 0.3, respectively. Further, let the threshold value ρ_{th} be 0.5 for classifying critical data from normal data. In this scenario, $\mathfrak{J}_p^{min}$ for WBAN p is determined to be 2 (based on Table 5.1), i.e., the sum of the required PRBs for transmitting blood saturation and body temperature sensors' data. Meanwhile, $\mathfrak{J}_p^{max}$ for WBAN p becomes 4, i.e., the total required PRBs for transmitting all the three sensors' data.

5.2.2 PRB Allocation Model

Let $\mathbb{N} = \{1, \ldots, n, \ldots, N\}$ be the set of available PRBs in 5G network. Further, we introduce a binary variable that shows PRB allocation relation between WBAN and UAV as:

$$y_{p,u}^{n} = \begin{cases} 1, & \text{if } n^{th} \text{ PRB is allocated to } (p,u); \\ 0, & \text{otherwise.} \end{cases} \tag{5.3}$$

Each UAV has a coverage area, that can also be considered as UAV's transmission range, and it is possible for two coverage areas to overlap. Let Φ_u be the set of all WBANs within the coverage area of UAV u. Interference among the WBANs can occur in the network if same PRB is assigned to two WBANs p and p' that are within the coverage area of a UAV, as shown in Fig. 5.2. However, the above condition could be avoided using the following constraints for a given n^{th} PRB:

(C_1) Ensure $\sum_{p \in \Phi_u} y_{p,u}^{n} \leq 1, \forall\ u \in \mathbb{U}$.

In other words, the interference can be avoided if no two WBANs within a coverage area of a UAV are allocated the same PRB, as stated above in (C_1).

5.2.3 Energy Consumption of WBAN

To facilitate the data transmission, the required number of PRBs must be allocated to WBANs. The data rate between WBAN p and UAV u using PRB n is given as follows [15]:

$$\mathrm{r}_{p,u}^{n} = \omega \log_2 \left(1 + \jmath_{p,u}^{n}\right), \tag{5.4}$$

where ω and $\jmath_{p,u}^{n}$ are bandwidth of a PRB and SINR[5] between WBAN p and UAV u while using PRB n, respectively. Then, the achievable data rate between WBAN p and UAV u is given as follows:

$$\mathbb{R}_{p,u} = \sum_{n \in \mathbb{N}} y_{p,u}^{n}\ \mathrm{r}_{p,u}^{n}. \tag{5.5}$$

[5]In this chapter, we modeled the interference among WBANs based on our previous work [15].

Thus, transmission time between WBAN p and UAV u can be defined as follows [120]:

$$\mathrm{K}_p^{tr,u} = \frac{\eta_p}{\mathbb{R}_{p,u}}, \tag{5.6}$$

where η_p is the size of physiological data to be transmitted by WBAN p. Thus, energy consumed by WBAN p for transmitting physiological data to UAV u is defined as follows:

$$\mathrm{E}_p^{tr,u} = \varpi_p \mathrm{K}_p^{tr,u}, \tag{5.7}$$

where ϖ_p is the transmit power of WBAN p.

To prioritize the transmission of critical data, a priority parameter φ_p is introduced, which characterizes the criticality of physiological data and the energy consumption rate of the WBAN. Mathematically, the priority parameter φ_p is defined as the weighted average of the criticality and the energy consumption of WBAN p, as follows [38]:

$$\varphi_p = \frac{b_1\rho_p + b_2 E_p}{b_1 + b_2}, \tag{5.8}$$

where ρ_p represents the criticality of WBAN p (discussed in Eq. (3.3) of Chapter 3), $E_p = \sum_{u\in\mathbb{U}} \mathrm{E}_p^{tr,u}/\mathrm{E}_p^{init}$, and E_p^{init} is the initial energy of WBAN p [38]. b_1 and b_2 are positive weights such that $b_1 + b_2 = 1$. The value of φ_p lies between 0 and 1, i.e., $0 \leq \varphi_p \leq 1$, with a higher φ_p indicating that the physiological data of WBAN p is highly critical, and vice versa.

5.2.4 Revenue of WBAN

Model owner provides reward to WBAN for transmitting physiological data to UAV based on the number of physiological data samples. Let D_p be the number of physiological data samples available at WBAN p, then, the reward of WBAN p from the

model owner is defined as follows [122]:

$$\mathfrak{R}_p = \mathfrak{d} D_p, \tag{5.9}$$

where $\mathfrak{d}$ is the price per physiological data sample. Thus, the revenue of WBAN p for transmitting physiological data to UAV u is defined as follows:

$$\Theta_{p,u} = \mathfrak{R}_p - \alpha_p \mathrm{E}_p^{tr,u}, \tag{5.10}$$

where α_p represents the unit cost of energy for a WBAN. Therefore, total revenue of all WBANs is defined as follows:

$$\mathbb{A} = \sum_{p \in \mathbb{P}} \sum_{u \in \mathbb{U}} \Theta_{p,u}. \tag{5.11}$$

5.2.5 UAV Data Collection

UAVs are tasked by the model owner to collect physiological data from WBANs. Subsequently, UAVs travel to a predetermined position in the region[6] assigned by the model owner with velocity v_u, and spend a fixed propulsion power, given by: $\mathrm{p}_u = \mathscr{e}_u^{pd}(\mathrm{v}_u)^3 + \frac{\mathscr{e}_u^{rd}}{\mathrm{v}_u}$, where $\mathscr{e}_u^{pd}$ represents power to balance skin friction parasitic drag, and $\mathscr{e}_u^{rd}$ represents power to balance redirection drag force of air[7] [10]. Let L_u be the distance travelled by UAV u from its base to the assigned region, known as *traversal distance*, then, the time taken by the UAV for traversal is given by: $\mathfrak{z}_u^{tve} = \frac{\mathrm{L}_u}{\mathrm{v}_u}$. Thus, the energy consumption of UAV u during traversal is given by:

$$\mathrm{E}_u^{tve} = \mathrm{p}_u \mathfrak{z}_u^{tve}. \tag{5.12}$$

[6]Region selection and path finding of UAVs are outside the scope of this chapter. However, region selection and path finding of UAVs can be done using the methods given in [10] and [123], respectively.

[7]The propulsion power consumed by the UAV when it changes its direction is negligible [10].

After reaching the assigned region, UAVs receive physiological data from WBANs within their coverage area. The energy consumed by UAV u while receiving[8] physiological data of WBAN p is calculated as follows [125]:

$$\mathrm{E}_{u,p}^{rec} = \frac{\mathbb{R}_{p,u}}{\imath \varpi_p + P_{cir}}, \tag{5.13}$$

where P_{cir} represents the circuit's power consumption, including the power consumption of the mixer, frequency synthesizer, and digital-to-analog converter. $\imath > 1$ is a constant that depends on the efficiency of the power amplifier [125]. Thus, the total energy consumption of UAV u for traversal and receiving physiological data is defined as follows:

$$\mathrm{E}_{u}^{tot} = \mathrm{E}_{u}^{tve} + \sum_{p \in \mathbb{P}} \mathrm{E}_{u,p}^{rec}. \tag{5.14}$$

5.2.6 UAV Model Training

After receiving physiological data from WBANs, UAVs return to the UAV base[9] and collaboratively train an FL model [10]. Let vector $\mathbf{w}^{(i)}$ be the parameter of the FL model at global iteration i. In each global iteration, there are three steps involved [10,49,117]: (i) *Local Model Training*: UAV trains the local model using global parameter $\mathbf{w}^{(i)}$, (ii) *Local Model Transmission*: UAV transmits the model parameter[10] to the MBS, and (iii) *Global Model Aggregation*: MBS aggregates all parameters from UAVs to get a global model parameter $\mathbf{w}^{(i+1)}$, which is then transmitted back to the UAVs for the $(i+1)^{th}$ global iteration. In general, each UAV solves the local optimization problem $\mathfrak{G}_u$ given in the following:

$$\min_{\mathfrak{h}_u \in \mathbb{R}^d} \mathfrak{G}_u\left(\mathbf{w}^{(i)}, \mathfrak{h}_u\right) \triangleq \mathfrak{F}_u\left(\mathbf{w}^{(i)} + \mathfrak{h}_u\right) - \nabla \mathfrak{F}_u\left(\mathbf{w}^{(i)}\right) - \lambda \nabla \mathfrak{F}_u\left(\mathbf{w}^{(i)}\right)^T \mathfrak{h}_u, \tag{5.15}$$

[8]This chapter did not consider the hovering energy of UAVs during the collection of physiological data from WBANs; nevertheless, it can be easily extended to include hovering energy [124].

[9]We assume that the UAV base has an abundant supply of energy.

[10]Mitigating privacy risks associated with attackers reconstructing raw data from model parameters is beyond the scope of this chapter. However, this can be addressed using the methods given in [29,126].

where $\measuredangle$ is a constant value. A solution $\mathfrak{h}_u$ to Eq. (5.15) denotes the difference between the global model at the MBS and the local model at UAV u, i.e., the local model parameter at UAV u is $(\mathbf{w}^{(i)} + \mathfrak{h}_u)$ [112]. Each UAV performs local model training multiple times to minimize L-Lipschitz and $\mathfrak{i}$-strong convex loss function $\mathfrak{G}_u$ to achieve target training accuracy $\mathcal{A}$, which is defined by the model owner. A higher value of target accuracy $\mathcal{A}$ indicates a greater deviation from the optimal solution. The optimization problem at UAV required $\mathfrak{v}\log_2(1/\mathcal{A})$ local iterations for model training to achieve local accuracy of $\mathcal{A}$ [10]. After $I = \frac{\mathrm{V}}{1-\mathcal{A}}$ global iterations, the entire FL model training process is completed. Here, $\mathrm{V} = \frac{2L^2}{\mathfrak{i}^2\mathrm{Y}}$ and Y is a very small value that satisfies the following constraint: $0 \leq \mathrm{Y} \leq \frac{\mathfrak{i}}{L}$. Let $\mathfrak{c}_u$ and $\mathfrak{b}_u$ be the computation capacity (CPU cycles per second) of UAV u and the CPU cycles per bit for computing one data sample at UAV u, respectively. Then, the energy consumption of UAV u for local model training using WBAN p's data is defined as follows [10]:

$$\mathfrak{E}_{u,p}^{com} = I\left(\psi \mathfrak{b}_u \mathfrak{v}\log_2(1/\mathcal{A})\mathfrak{c}_u^2\right) D_p, \tag{5.16}$$

where ψ is the effective capacitance that depends on the chip architecture [112], and $\mathfrak{v} = \frac{2}{(2-L\mathfrak{l})\mathfrak{l}\mathfrak{i}}$, where $\mathfrak{l}$ is the step size of model training. Thus, the energy consumption of UAV u for local model training is as follows:

$$\mathrm{E}_u^{com} = \sum_{p\in\mathbb{P}}\sum_{n\in\mathbb{N}} y_{p,u}^n \ \mathfrak{E}_{u,p}^{com}. \tag{5.17}$$

5.2.7 UAV Model Transmission

After model training, UAV transmits its model parameter to MBS for aggregation [10]. Transmission time of UAV to transmit its model parameter of size H is as follows [120]:

$$\tau_u^{tnt} = \mathfrak{r} I H l_u, \tag{5.18}$$

where $\mathfrak{r}$ is the transmission time to send one data unit across a unit distance, and l_u is the distance between the UAV base and the MBS. The size of local model remains constant, independent of the number of global iterations or the quantity of data. Then, the transmission energy of a UAV with transmit power of $\mathfrak{j}_u$ is defined as follows [10]:

$$\mathrm{E}_u^{tne} = \mathfrak{j}_u \tau_u^{tnt}. \tag{5.19}$$

5.2.8 Revenue of UAV

WBANs' physiological data collected by UAVs help the MBS develop a better inference model. Specifically, the model's accuracy in inference time is improved when the number of data samples increases, i.e., an FL model accuracy increases when the model is trained using a wide range of physiological data collected from WBANs. Inspired by [10,49,122], the reward function for UAVs in FL model training is defined based on the collected physiological data from WBAN p and its criticality, as given below:

$$\mathcal{J}_p = \ln(1 + D_p + \varphi_p). \tag{5.20}$$

Thus, the total reward of a UAV u is given as follows:

$$\mathscr{R}_u = \mathfrak{e}_u \sum_{p \in \mathbb{P}} \sum_{n \in \mathbb{N}} y_{p,u}^n \mathcal{J}_p, \tag{5.21}$$

where $\mathfrak{e}_u$ is the predefined non-zero positive number [122]. Thus, the revenue of a UAV u is defined as follows:

$$O_u = \mathscr{R}_u - \mathfrak{f}_u(\mathrm{E}_u^{tot} + \mathrm{E}_u^{com} + \mathrm{E}_u^{tne}), \tag{5.22}$$

where $\mathfrak{f}_u$ represents the unit cost of energy for UAV. Therefore, the total revenue of all UAVs is defined as follows:

$$\mathbb{B} = \sum_{u \in \mathbb{U}} O_u. \tag{5.23}$$

5.3 Problem Formulation

In the proposed architecture, WBANs get rewarded by the MBS based on the number of physiological data samples they transmit. Moreover, UAVs also aim to maximize their revenue by participating in FL training. Therefore, we define the total revenue as a linear combination of the revenues of WBANs and UAVs, as follows:

$$\mathcal{X} = \mathbb{A} + \mathbb{B}. \tag{5.24}$$

Thus, this chapter aims to maximize system revenue by allocating PRBs to WBANs for transmitting physiological data while minimizing interference and considering the priority of data. However, the total revenue of WBANs and UAVs should not exceed the model owner's maximum budget $\mathfrak{C}$. Therefore, the objective of the system is given as follows:

$$\textbf{P3:} \max_{y^n_{p,u}} \quad \mathcal{X}, \tag{5.25}$$

Subject to the constraints:

$$\Theta_{p,u} \geq 0, O_u \geq 0, \tag{5.25a}$$

$$\sum_{p \in \mathbb{P}} \sum_{u \in \mathbb{U}} \sum_{n \in \mathbb{N}} y^n_{p,u} \big(\mathfrak{R}_p + \mathscr{R}_u\big) \leq \mathfrak{C}, \tag{5.25b}$$

$$\mathfrak{J}^{min}_p \leq \sum_{n \in \mathbb{N}} y^n_{p,u} \leq \mathfrak{J}^{max}_p, \tag{5.25c}$$

$$\sum_{p \in \Phi_u} y^n_{p,u} \leq 1, \tag{5.25d}$$

$$y^n_{p,u} \in \{0, 1\}, \tag{5.25e}$$

$\forall p, p' \in \mathbb{P}, u \in \mathbb{U}, n \in \mathbb{N}$. Constraint in Eq. (5.25a) states that the revenue of WBANs and UAVs must be non-negative. Constraint in Eq. (5.25b) tells that the total reward given to WBANs and UAVs should not exceed the maximum budget of the model owner. Constraint in Eq. (5.25c) ensures minimum and maximum required PRBs for a WBAN. Constraint in Eq. (5.25d) holds the interference criteria described in (C_1) of Subsection 5.2.2. Constraint in Eq. (5.25e) is the binary variable given in Eq. (5.3).

The objective of the proposed problem **P3** is computationally hard to solve. However, constraint in Eq. (5.25d) allows us to construct an interference graph, that MBS uses to allocate PRBs across different WBANs without causing interference. Moreover, Fig. 5.3 shows the data flow between WBAN, UAV, and MBS. Labels 1, 2, 3, 5, 7, and 9 are handled by control signals (e.g., beacons [15]). However, labels 4, 6, and 8 are handled by data signals. The formulated problem **P3** can be considered as a graph coloring problem by mapping PRB with color in graph topology as described in the following.

5.3.1 Interference Graph Construction

We create an interference graph $\mathrm{G}(\mathbb{V}, \mathbb{E})$ from the WBAN topology where vertex $v \in \mathbb{V}$ and edge $e \in \mathbb{E}$ represent WBANs and interference between two WBANs, respectively. In other words, any two interfering WBANs have an edge between them in the graph G. The graph G satisfies the constraint in Eq. (5.25d). Fig. 5.2 shows a WBAN topology and the respective interference graph. Moreover, we assume that MBS maintains the interference graph.

Theorem 5.1 *Formulated maximization problem **P3** is NP-hard.*

Proof: We map the graph κ-coloring problem to the formulated problem **P3**, where κ is the total number of colors. For simplicity, we consider $\mathfrak{J}_p^{min} = \mathfrak{J}_p^{max} = 1$ and ignore the constraints (5.25a)-(5.25c) to prove the hardness of the problem.

- Map the set of κ-colors to N PRBs.

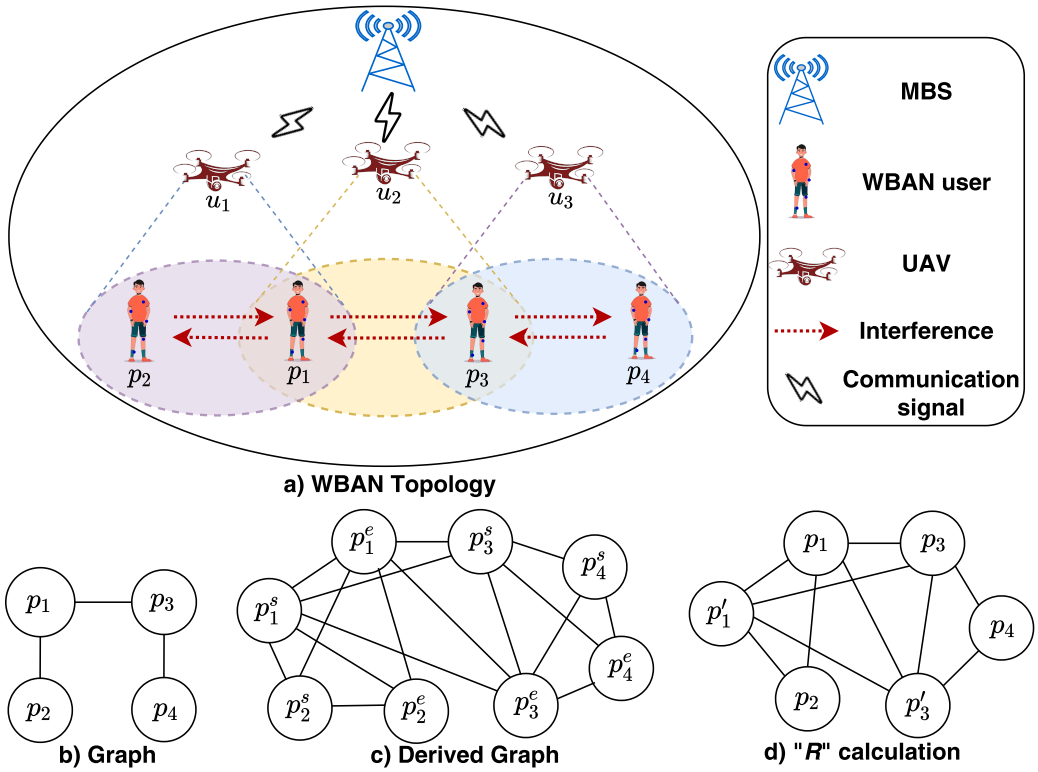

Fig. 5.2. WBAN topology and interference graph.

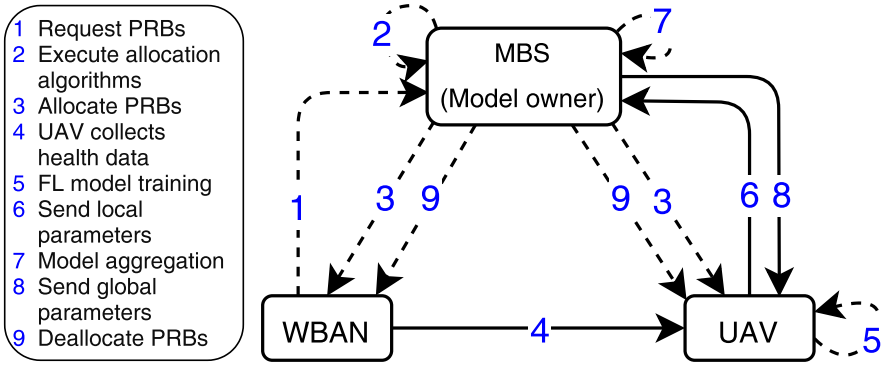

Fig. 5.3. Data flow diagram.

- Map the set of vertices, $\mathbb{V}$, to the set of WBANs, $\mathbb{P}$.
- Map the set of edges, $\mathbb{E}$, to interference constraints.
- Map the interference graph to the WBAN topology.

Table 5.2 shows the mapping of the RA problem to the vertex κ-coloring, which is NP-complete [127], implying the formulated problem **P3** is an NP-hard. □

Table 5.2: κ-coloring & RA

Vertex coloring	**RA**
Set of κ colors	Set of N PRBs
Set of vertices, $\mathbb{V}$	Set of WBANs, $\mathbb{P}$
Set of edges, $\mathbb{E}$	Interference constraints
Graph G	WBAN topology

Due to the high dimensionality and ill-posed nature of problem **P3**, we aim to solve the formulated problem via RA in UAV-assisted WBANs underlying 5G. We applied a matching and graph coloring-based approach to solve the formulated problem in computationally feasible time while satisfying the varying PRB demand, limited PRBs, and a large number of WBANs within the coverage area of UAVs.

5.4 Matching and Graph Coloring based RA

The conventional matching theory of buyer/seller is not applicable in the WBAN scenario. Buyers and sellers express their preferences for various sellers and buyers based on a preference list that is reflexive, complete, and transitive in relation. However, the preference list defined for buyer/seller is not sufficient for RA in WBAN-based scenarios due to the reusability of PRBs [31, 55]. To address this problem, we use the concept of the preference list of WBANs over UAV-PRB pairs, and vice-versa. Intuitively, WBAN prefers a UAV-PRB pair with the highest transmission rate. Thus, the preference list of WBAN p over UAV u using PRB n is constructed based on the data transmission rate. Let $\mathbb{K}$ be the set of UAV-PRB pairs denoted as $\mathbb{K} = \{(u, n)|\forall u \in \mathbb{U}, \forall n \in \mathbb{N}\}$. In the rest of the chapter, we use k_u^n to denote (u, n) pair for simplicity. Then, the preference list of WBAN p can be expressed as follows:

$$\mathrm{k}_u^n \succeq_p \mathrm{k}_{u'}^n \Leftrightarrow \mathrm{r}_{p,u}^n \geq \mathrm{r}_{p,u'}^n. \tag{5.26}$$

We assume that the PRB related information is available to MBS, and the functionality of PRB is monitored by MBS [15].

On the other hand, UAVs always consider the revenue when selecting WBANs to match. If $\mathbb{T}, \mathbb{Q} \subseteq \mathbb{P}$ denote two subsets of WBANs, then UAV-PRB pair k_u^n prefers $\mathbb{T}$ to $\mathbb{Q}$ if: (i) Total revenue for collection of data from WBANs in group $\mathbb{T}$ is larger than that of group $\mathbb{Q}$, and $\mathbb{T}$ contains only non-interfering WBANs, or (ii) $\mathbb{T}$ contains only non-interfering WBANs but $\mathbb{Q}$ does not, as defined below:

$$\mathbb{T} \succeq_{\mathrm{k}_u^n} \mathbb{Q} \Leftrightarrow$$
$$\begin{cases} (i)\ \forall p, p' \in \mathbb{T}, e_{p,p'} = 0, \forall p, p' \in \mathbb{Q}, e_{p,p'} = 0, & \sum_{p\in\mathbb{T}}\{\mathcal{J}_p - \mathfrak{f}_u(\mathrm{E}_{u,p}^{rec} + \mathfrak{E}_{u,p}^{com})\} \geq \\ & \sum_{p\in\mathbb{Q}}\{\mathcal{J}_p - \mathfrak{f}_u(\mathrm{E}_{u,p}^{rec} + \mathfrak{E}_{u,p}^{com})\}; \\ (ii)\ \exists p, p' \in \mathbb{Q}, e_{p,p'} = 1, & \text{otherwise}, \end{cases} \tag{5.27}$$

where $e_{p,p'} = 1$ indicates the edge between WBANs p and p' in the graph G, which means WBANs p and p' are interfering with each other. Contrary, if $e_{p,p'} = 0$, there is no edge between WBANs p and p' in the graph G, which means they are non-interfering WBANs. Note that MBS maintains the preference list of UAV-PRB pairs. Based on the above discussion, we define matching in the following.

Definition 5.1 *A feasible resource matching μ is defined as a function, i.e., $\mu : \mathbb{P} \cup (\mathbb{U} \times \mathbb{N}) \rightarrow 2^{\mathbb{P}} \cup 2^{\mathbb{U}\times\mathbb{N}}$ such that:*

(I) $\forall \mathrm{k}_u^n \in \mathbb{K}, \mu(\mathrm{k}_u^n) \subseteq \mathbb{P}$ and $\forall p \in \mathbb{P}, \mu(p) \subseteq \mathbb{K}$.

(II) $\forall \mathrm{k}_u^n \in \mathbb{K}$ and $\forall p \in \mathbb{P}, \mathrm{k}_u^n \in \mu(p) \Leftrightarrow p \in \mu(\mathrm{k}_u^n)$.

(III) Interference constraint: $\forall p, p' \in \mu(\mathrm{k}_u^n)$, $e_{p,p'} = 0$.

(IV) $\forall p \in \mathbb{P}, \mathfrak{J}_p^{min} \leq |\mu(p)| \leq \mathfrak{J}_p^{max}$.

5.4.1 Resource Allocation Algorithm

Each WBAN requires a minimum allocation of PRBs to prioritize critical data transmission. To facilitate this, each WBAN is divided into two dummy WBANs - *steady* and *elaborate*. Steady and elaborate WBANs handle the minimum and the maximum requirements, respectively. Let p^s and p^e be steady and elaborate WBANs of WBAN p, respectively, then, we transform the minimum requirement into maximum requirements of steady and elaborate WBANs such as $\mathfrak{J}_{p^s}^{max} = \mathfrak{J}_p^{min}$ and $\mathfrak{J}_{p^e}^{max} = \mathfrak{J}_p^{max} - \mathfrak{J}_p^{min}$, respectively. Moreover, reserving $\sum_p \mathfrak{J}_p^{min}$ PRBs can guarantee resources for steady WBANs, and the remaining $R = N - \sum_p \mathfrak{J}_p^{min}$ can be allocated to elaborate WBANs.

We follow the Deferred Acceptance Algorithm (DAA) for school admission problem [30], wherein a set of students apply for admission to a college having a maximum quota. A school has a quota of $\mathfrak{J}^{max}$, keeps top $\mathfrak{J}^{max}$ students in a list, or all the applicants if the number of students is less than $\mathfrak{J}^{max}$; others get rejected. Further, rejected students apply to other schools that have never disqualified them. Thus, the school shortlists top $\mathfrak{J}^{max}$ students from the current list and previous waiting list. These steps continue until each student has exhausted the schools that s/he can apply for. In our case, we follow the scenario where UAV-PRB pairs propose and WBANs either accept or reject them as they must fulfill the minimum and maximum demand. Further, we transform the minimum resource demand of WBANs into resource matching without the minimum resource demand using Algorithm 5.1 in the following.

1) Derived Resource Matching: Algorithm 5.1 transforms minimum resource demand of WBANs into resource matching without minimum resource demand. In the transformed matching, the number of resources N remains unchanged, and preference lists of steady and elaborate WBANs remain the same as the original WBAN (line 5). The preference list of resource pairs is redefined by placing elaborate WBANs immediately after steady WBANs, preserving the initial preference order (line 8). The resulting interference graph $\hat{\mathrm{G}}(\hat{\mathbb{V}}, \hat{\mathbb{E}})$ includes steady and elaborate nodes for each WBAN in G,

Algorithm 5.1: Derived Resource Matching Algorithm

Input: $\mathbb{P}, \mathbb{K}$, Preference list $\succeq_p, \forall p \in \mathbb{P}$, $\succeq_{\mathrm{k}_u^n}, \forall \mathrm{k}_u^n \in \mathbb{K}$, $\mathfrak{J}_p^{min}$, $\mathfrak{J}_p^{max}, \forall p \in \mathbb{P}$, $\mathrm{G}(\mathbb{V}, \mathbb{E})$

Output: WBAN set $\hat{\mathbb{P}}$, preference list of WBANs $\hat{\succeq}_p, \forall p \in \hat{\mathbb{P}}$, preference list of UAV-PRB pair $\hat{\succeq}_{\mathrm{k}_u^n}, \forall \mathrm{k}_u^n \in \mathbb{K}$, maximum demand $\hat{\mathfrak{J}}_p^{max}$, $\forall p \in \hat{\mathbb{P}}$, derived interference graph $\hat{\mathrm{G}}(\hat{\mathbb{V}}, \hat{\mathbb{E}})$

1 $\hat{\mathbb{P}}^s = \varnothing, \hat{\mathbb{P}}^e = \varnothing$
2 **for** *all* $p \in \mathbb{P}$ **do**
3 $\quad \hat{\mathbb{P}}^s = \hat{\mathbb{P}}^s \cup \{p^s\}$, $\hat{\mathbb{P}}^e = \hat{\mathbb{P}}^e \cup \{p^e\}$
4 $\quad \mathfrak{J}_{p^s}^{max} = \mathfrak{J}_p^{min}, \mathfrak{J}_{p^e}^{max} = \mathfrak{J}_p^{max} - \mathfrak{J}_p^{min}$
5 $\quad$ Preference list of steady and elaborate WBANs: $\hat{\succeq}_{p^s} := \hat{\succeq}_{p^e} := \succeq_p$
6 $\hat{\mathbb{P}} = \hat{\mathbb{P}}^s \cup \hat{\mathbb{P}}^e$
7 **for** *all* $\mathrm{k}_u^n \in \mathbb{K}$ **do**
8 $\quad$ Change $\succeq_{\mathrm{k}_u^n} := k_{\mathrm{k}_u^n,1} \succeq_{\mathrm{k}_u^n} k_{\mathrm{k}_u^n,2} \succeq_{\mathrm{k}_u^n} \ldots$, into $\hat{\succeq}_{\mathrm{k}_u^n} := p^s_{\mathrm{k}_u^n,1} \hat{\succeq}_{\mathrm{k}_u^n} p^e_{\mathrm{k}_u^n,1} \hat{\succeq}_{\mathrm{k}_u^n} p^s_{\mathrm{k}_u^n,2} \hat{\succeq}_{\mathrm{k}_u^n} p^e_{\mathrm{k}_u^n,2} \hat{\succeq}_{\mathrm{k}_u^n} \cdots$
9 $\quad$ **for** *all node* $p \in \mathrm{G}$ **do**
10 $\quad\quad$ Add p^s and p^e to $\hat{\mathbb{V}}$ of $\hat{\mathrm{G}}$
11 $\quad\quad$ p^s and p^e inherits all the edges of p to $\hat{\mathbb{E}}$ of G
12 $\quad\quad$ Create an edge between p^s and p^e

Algorithm 5.2: Minimum Resource Requirement

Input: $\mathfrak{J}_p^{min}, \forall p \in \mathbb{P}, \mathrm{G}(\mathbb{V}, \mathbb{E}), \mathbb{P}, \mathbb{N}$, a set $\mathfrak{L} := \varnothing$

Output: R

1 **for** *all node* $p \in \mathrm{G}$ **do**
2 $\quad$ Create clique of size $\mathfrak{J}_p^{min}$
3 $\quad$ Each node of clique $\mathfrak{J}_p^{min}$ inherits all the edges of $p \in \mathrm{G}$ and a new graph $\mathrm{G}'(\mathbb{V}', \mathbb{E}')$ is created w.r.t. the requirements of steady WBANs
4 **while** $\mathbb{V}'$ *is not empty* **do**
5 $\quad$ Remove a node p from $\mathbb{V}'$
6 $\quad$ Allocate resource $n \in \mathbb{N}$, which is not allocated to any one hop of node p
7 $\quad \mathfrak{L} = \mathfrak{L} \cup \{n\}$
8 $R = N - |\mathfrak{L}|$

inheriting all edges along with an edge between them to avoid sharing the same PRB (lines 9-12). The output of Algorithm 5.1 is used as input of Algorithm 5.3.

2) Minimum Resource Requirement: Algorithm 5.2 evaluates the minimum required PRBs for steady and elaborate WBANs by applying the graph coloring technique. A virtual clique of size $\mathfrak{J}^{min}$ is generated to account for multiple PRB requests per WBAN

Algorithm 5.3: Resource Matching Algorithm

Input: Outputs of Algorithms 5.1 and 5.2; $\Theta_{p,u}, O_u, \mathfrak{C}$, $y^n_{p,u} = 0$, $\mathfrak{R}_p, \mathscr{R}_u$, $\forall p \in \mathbb{P}, \forall u \in \mathbb{U}, \forall n \in \mathbb{N}$

Output: Resource matching $\hat{\mu}$, revenue $\mathcal{X}$

1 $\forall p \in \hat{\mathbb{P}}, \hat{\mu}(p) = \varnothing$, waiting list $\mathrm{W}_p = \varnothing; \forall \mathrm{k}^n_u \in \mathbb{K}$, $\hat{\mu}(\mathrm{k}^n_u) = \varnothing$, candidate list $C_{u,n} = \hat{\mathbb{P}}$, $\hat{\mathbb{N}} = \mathbb{N}$
2 **while** $\exists C_{u,n} \neq \varnothing$ **do**
3 **for** *all resource pair* k^n_u *with* $|C_{u,n}| > 0$ **do**
4 $\mathscr{Z}_{u,n}$:= WBANs that satisfies $p \in C_{u,n}$; $\forall p' \in \mu(\mathrm{k}^n_u), e_{p,p'} = 0$
5 Find MWIS on $\mathscr{Z}_{u,n}$ as $\mathscr{Z}^{max}_{u,n}$
6 **if** $\forall \mathrm{k}^n_u, \mathscr{Z}^{max}_{u,n} = \varnothing$ **then**
7 Return $\hat{\mu}$
8 **else**
9 **for** *all WBAN* $p \in \mathscr{Z}^{max}_{u,n}$ **do**
10 **if** *Constraints* (5.25a) *and* (5.25b) *are met* **then**
11 Resource k^n_u applies for WBAN p
12 $C_{u,n} = C_{u,n} - \{p\}, \mathrm{W}_p = \mathrm{W}_p \cup \{\mathrm{k}^n_u\}$
13 **for** *all WBAN* p *for which* $\mathrm{W}_p \neq \varnothing$ **do**
14 **if** $p \in \hat{\mathbb{P}}^s$ **then**
15 p accepts $\mathfrak{J}^{max}_p$ resources in $\mathrm{W}_p \cup \hat{\mu}(p)$, and set $\mathrm{W}_p = \varnothing$, $y^n_{p,u} = 1$
16 **else**
17 $cnt = 0$
18 **for** *all* $p \in \hat{\mathbb{P}}^e$ **do**
19 $\mathrm{W}_p = \mathrm{W}_p \cup \mu(p), \mu(p) = \varnothing$
20 **while** $cnt < R$ *and* $\exists p^e, \mathrm{W}_{p^e} \neq \varnothing$ *and* $|\hat{\mu}(p^e)| < \hat{\mathfrak{J}}^{max}_{p^e}$ **do**
21 **if** $|\mu(p^e)| < \hat{\mathfrak{J}}_{p^e}$ *and* $\mathrm{W}_{p^e} \neq \varnothing$ **then**
22 p^e selects its most preferred k^n_u in W_{p^e}, such that $\hat{\mu}(p^e) = \hat{\mu}(p^e) \cup \{\mathrm{k}^n_u\}$
23 $y^n_{p,u} = 1$ for accepted resource pairs
24 $\mathrm{W}_{p^e} = \mathrm{W}_{p^e} - \{\mathrm{k}^n_u\}$
25 $cnt = cnt + 1$, $\hat{\mathbb{N}} = \hat{\mathbb{N}} - \{n\}$
26 $\mathrm{W}_p = \varnothing$
27 Calculate revenue $\mathcal{X}$ based on the matching $\hat{\mu}$

and inherits all the original edges of G, resulting in a new graph $\mathrm{G}'(\mathbb{V}', \mathbb{E}')$. A vertex is selected and assigned with a PRB that has not been assigned within one-hop distance of that vertex and updates in the set $\mathfrak{L}$ (lines 4-7). This process iterates for all vertices

in the graph. In the end, the set $\mathfrak{L}$ contains all the required PRBs for steady WBANs, and R denotes the number of required PRBs for elaborate WBANs. The output of Algorithm 5.2 is used as input of Algorithm 5.3 in the following.

3) Resource Matching Algorithm: Algorithm 5.3 uses different rules for steady and elaborate WBANs to accept or reject a resource pair. Let $C_{u,n}$ be the set of WBANs that a resource pair k_u^n has not yet applied. Line 1 initializes the required variables. In every round, each resource pair k_u^n selects a set of non-interfering WBANs $\mathscr{Z}_{u,n}$ (lines 3-4), and finds the Maximum Weighted Independent Set (MWIS) $\mathscr{Z}_{u,n}^{max}$ on the set $\mathscr{Z}_{u,n}$ (line 5). If $\mathscr{Z}_{u,n}^{max}$ becomes empty for all resource pairs, Algorithm 5.3 terminates (lines 6-7); otherwise, WBAN adds the resource pair to its waiting list (lines 9-12). A WBAN with a non-empty waiting list selects its required $\mathfrak{J}_{p^s}^{max}$ resources and resets its waiting list (lines 14-15).

Let *cnt* be counter to track the number of PRBs allocated to elaborate WBANs (line 17). Add each elaborate WBAN's matched resource to the waiting list and reset the matched resources (lines 18-19). If the number of PRBs allocated to elaborate WBANs is less than R, or there exists elaborate WBANs with a non-empty waiting list and do not fulfill their maximum demand, then WBAN p^e selects its most preferred UAV-PRB pairs from the waiting list until the maximum demand is reached or its waiting list is empty (lines 20-25). The counter value increases by one and returns to line 20. Finally, the waiting list of WBAN p is set to empty (line 26). This process repeats for all the resource pairs with non-empty set $C_{u,n}$ (lines 2-26). Therefore, we get the matching such as $\forall p \in \mathbb{P}, \mu(p) = \hat{\mu}(p^e) \cup \hat{\mu}(p^s), \forall \mathrm{k}_u^n \in \mathbb{K}$, if $p^e \in \hat{\mu}(\mathrm{k}_u^n)$ or $p^s \in \hat{\mu}(\mathrm{k}_u^n)$ then $p \in \mu(\mathrm{k}_u^n)$. Thus, the total revenue can be calculated based on the matching $\hat{\mu}$ (line 27).

5.4.2 Analysis of the Algorithms

We analyze the computational time complexity and the correctness of the proposed algorithm in the following.

Theorem 5.2 *Computational time complexity of proposed algorithm is* $O(NP^2U|\hat{\mathbb{V}}|^3)$.

Proof: The time complexity of Algorithm 5.1 is $O(PNU)$, and that of Algorithm 5.2 is $O(P)$. In Algorithm 5.3, each steady WBAN is approached by a UAV-PRB pair once, and N PRBs are allocated by examining the MWIS in the graph. To find out MWIS, each edge must be traversed, which takes $O(|\hat{\mathbb{E}}|)$ time complexity. This process repeats for all vertices in the derived interference graph, resulting in $O(|\hat{\mathbb{V}}||\hat{\mathbb{E}}|)$ time complexity, i.e., $O(|\hat{\mathbb{V}}|^3)$. Moreover, the number of MWIS is bounded by the total available PRBs, i.e., 100 [95]. Therefore, an approximate algorithm for MWIS takes $O(|\hat{\mathbb{V}}|^3)$ time complexity [95]. Thus, the time complexity for allocating PRBs to each steady WBAN is $O(PN|\hat{\mathbb{V}}|^3)$. Further, to allocate PRBs to an elaborate WBAN (lines 20-26 of Algorithm 5.3), all the remaining elaborate WBANs need to be visited, resulting in a time complexity of $O(P)$. Hence, time complexity of the proposed algorithm is $O(NP^2U|\hat{\mathbb{V}}|^3)$. □

Lemma 1 *For every WBAN* $p \in \mathbb{P}$*, the proposed algorithm produces an interference-free solution.*

Proof: To avoid interference, the proposed approach allocates different PRBs to WBANs within a one-hop distance of the interference graph. Algorithm 5.3 always examines already allocated PRBs within one hop of the particular vertex in the interference graph. This phenomenon is handled by finding the MWIS in the topology (line 5 of Algorithm 5.3). Thus, the proposed algorithm reuses the same PRBs only after the one-hop distance in the topology to ensure an interference-free network. Therefore, the proposed algorithm gives an interference-free RA for every WBAN. □

5.5 Performance Analysis

We evaluate the performance of our proposed algorithm using the publicly available Shanghai Telecom dataset [128, 129], which comprises data from 9481 mobile phone users across 3233 BSs. We select BSs within a 2000 m x 2000 m area to serve as UAVs with additional UAVs randomly placed in the same area to densify the network and simulate a 5G environment. We randomly select [100-1000] mobile phones to act as WBANs, and Fig. 5.4 presents a snapshot of the system at a specific time stamp. Each UAV has a coverage radius of 200 m [130]. It is worth noting that acquiring real-time user data across their BSs in cellular networks is challenging since operators usually keep such information confidential. The computation capacity of UAVs is set to 2 GHz [10], and the CPU cycles per bit for computing one data sample are uniformly chosen from [10-30] cycles. Physiological data size for WBANs ranges between [500-1000] MB, and the FL model size is set to 1 MB [10] (see Table 5.3). Minimum and maximum PRB demands of a WBAN ranges between [1-6]. Simulation is done using Python 3.9 on a Windows 10 Home PC equipped with an Intel® Core™ i7-10750H @ 2.60 GHz processor and 16 GB of memory.

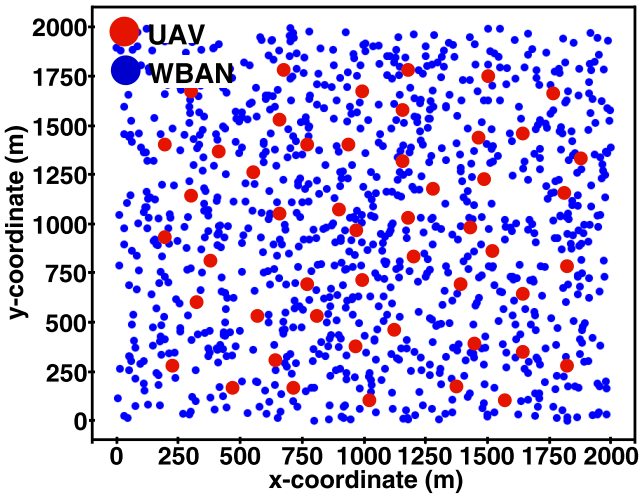

Fig. 5.4. Deployment scenario.

We compared our results with the existing works SSAA [52], CAA [51], and the *Optimal* value obtained using the *Gurobi* optimization tool [103], using the same simulation parameters. To the best of our knowledge, existing works SSAA and CAA are the closest works to our proposed architecture. Particularly, we compared our work with SSAA since it allocates channels to users while considering mutual interference and

Table 5.3: Details of simulation parameters

Parameter	Value
P, U, N [95]	[100-1000], [20-50], 100
$\mathfrak{J}_p^{min}, \mathfrak{J}_p^{max}$ [95]	$[1-6]$
Bandwidth [131], $\mathfrak{r}$	20 MHz, 1 unit
Deployment area [52]	2000 (m) x 2000 (m)
$\mathfrak{b}_u, \mathfrak{c}_u$ [10]	[10-30] cycles/bit, 2 GHz
ρ_p [3], $\mathfrak{e}_u$ [10], b_1, b_2, D_p	[0-1], 100000, 0.5, 0.5, 437
η_p [10], ϖ_p [112]	[500-1000] MB, [1-10] dB
$\mathfrak{d}, \alpha_p, \mathfrak{f}_u$	1 unit, 1 unit, 1 unit
p_u, $\mathfrak{v}$, $L, \mathrm{Y}, \mathfrak{l}$ [10]	[10-35], 4, 4, $\frac{1}{3}$, $\frac{1}{4}$
L_u, v_u [10]	[1000-2000] m, [10-20] m/s
$\mathfrak{j}_u$ [10], ψ [112], P_{cir} [125]	[8-18], 10^{-28}, 25 dBm
$\mathcal{A}, I, H$ [10], $l_u, \mathfrak{C}$	0.6, 24, 1 MB, 1000 m, 10^8

considers the maximum number of channels each IoT device can receive. In contrast, CAA allocates subchannels to IoT nodes using a matching theory-based approach. For a fair comparison, we considered IoT nodes in [52] and mobile users in [51] as WBANs.

Revenue Analysis: Fig. 5.5a compares the total revenue of our proposed algorithm with SSAA, CAA, and optimal in various scenarios. The proposed algorithm outperforms SSAA and CAA, achieving 92.8% of the optimal value compared to that of 86.6% and 76.6% for SSAA and CAA, respectively. The reason is that SSAA allocates resources to maximize the uplink capacity without considering the minimum required PRBs, while CAA only allows each user to have one resource. In contrast, the proposed algorithm reuses PRBs and assigns the best UAV-PRB pair, considering minimum and maximum PRB demand, resulting in higher revenue in polynomial time complexity. Moreover, the revenue becomes constant as the number of WBANs increases (beyond 800 WBANs) because no more demand of WBANs can be fulfilled without interfering with each other.

Fig. 5.5b compares total revenue of our proposed algorithm with SSAA, CAA, and optimal in various scenarios. As seen from the result, the revenue increases as the number of UAVs increases. The proposed algorithm achieves 93.6% to optimal value

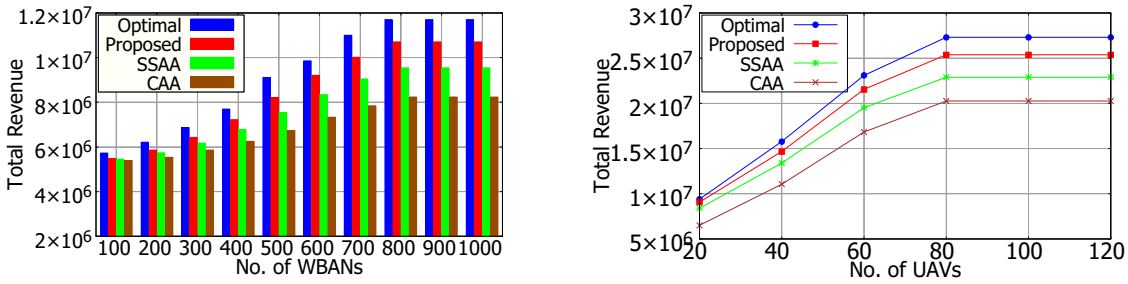

(a) Revenue (#UAV = 25) **(b)** Revenue (#WBAN = 1000)

Fig. 5.5. Revenue analysis.

compared to 85.0% and 72.4% for SSAA and CAA, on an average. The reason is that with an increasing number of UAVs, the resources are allocated more efficiently in the network, considering minimum and maximum demands of WBANs. This leads to lower transmission time, resulting in lower energy costs and higher revenue. In contrast, SSAA allocates resources to maximize the uplink capacity without considering the minimum required resources, while CAA only allows each user to obtain a single resource, leading to lower performance. Moreover, the revenue becomes constant as the number of UAVs increases (beyond 80 UAVs) because adding more UAVs introduces more interference, and no more demand of WBANs can be fulfilled without interfering with each other.

Fig. 5.6a presents three cases where the numbers of available PRBs are 80, 90, and 100, and the number of WBANs varies from 100 to 1000. The result shows that the revenue increases with an increase in the number of WBANs, indicating that more WBANs' demands are met with the given PRBs, resulting in higher revenue. However, the revenue growth slows down and becomes constant as the number of WBANs increases beyond a certain point because meeting more WBANs' demands lead to interference, negatively impacting the revenue. Additionally, increasing the number of PRBs allows more WBANs' demands to be met, leading to lower transmission costs and higher revenue.

In Fig. 5.6b, the total revenue is compared for varying FL model accuracies, ranging

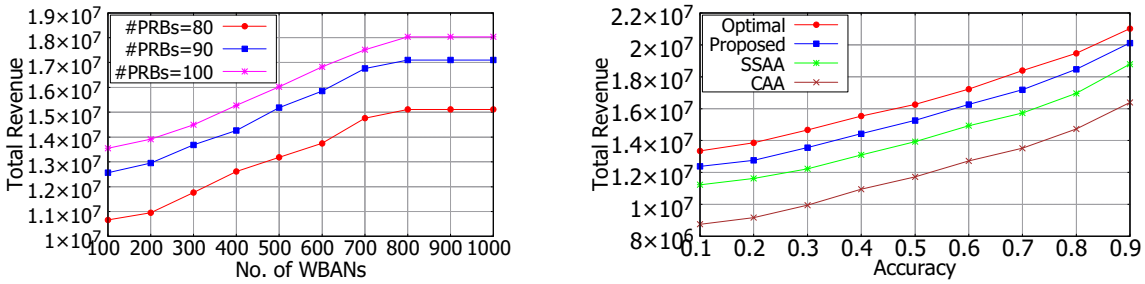

(a) Revenue vs. No. of WBANs **(b)** Revenue vs. accuracy

Fig. 5.6. Revenue based on number of WBANs and accuracy.

from 0.1 to 0.9, indicating a gradual decrease in accuracy. Numbers of WBANs and UAVs are fixed at 500 and 50, respectively. The proposed algorithm achieves 93.6% of the optimal value, compared to that of 85.5% for SSAA and 71.5% for CAA, on an average. We also observe that the revenue increases as the desired accuracy decreases. The reason is that achieving lower accuracy requires fewer local iterations, which results in lower energy consumption and leads to higher revenue.

Reuse Ratio Analysis: We compare PRB reuse ratio of the proposed algorithm with SSAA, and CAA. PRB reuse ratio refers to the ratio of the number of PRB that are reused in the network, to the total number of available PRBs [131].

Fig. 5.7a analyzes the impact of the number of WBANs over PRB reuse ratio in the system. The proposed algorithm outperforms SSAA, and CAA in terms of PRB reuse ratio. The reason is that SSAA allocates the resources to maximize the uplink capacity without considering the minimum required PRB, while CAA allocates only one resource to each user without considering the number of PRB demand of WBANs. Further, PRB reuse ratio obtained by the proposed algorithm is lower than that of the optimal because the optimal solution considers all possible combinations of allocations and selects the best out of them.

System Data Rate Analysis: Fig. 5.7b compares the system data rate achieved by our proposed algorithm with SSAA, CAA, and optimal value. The proposed al-

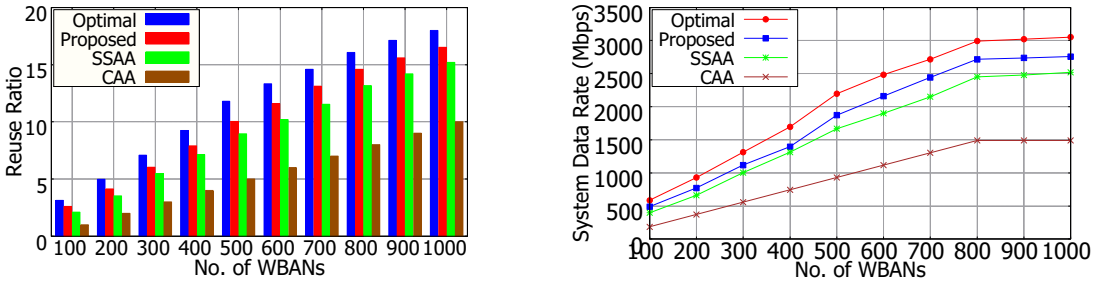

(a) Reuse ratio vs. WBANs **(b)** System data rate

Fig. 5.7. Reuse ratio and system data rate analysis.

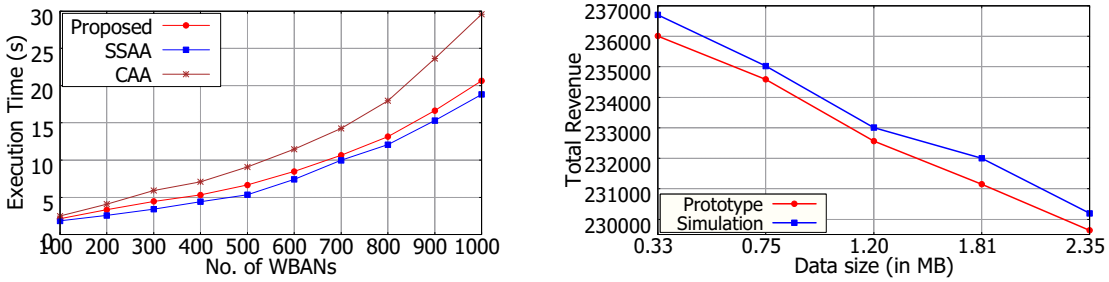

(a) Execution time **(b)** Prototype implementation

Fig. 5.8. Execution time and prototype model analysis.

gorithm outperforms SSAA and CAA in terms of system data rate. The reason is that with an increasing number of UAVs, resources are allocated more efficiently in the network by considering interference among WBANs, leading to a higher data rate. The results also show that the system data rate increases with an increasing number of WBANs, indicating that more WBANs' demands are met using the given PRBs. However, the data rate becomes constant as the number of WBANs increases beyond a certain point. This is because meeting more WBANs' demands leads to interference, preventing further increases in data rate without interference.

Execution Time Analysis: Fig. 5.8a compares the execution time of our proposed algorithm with SSAA, and CAA in various scenarios. As seen from the result, the execution time increases as the number of WBANs increases. The reason is that as the number of WBANs increases, the number of RA also increases, leading to longer

execution times. We also observe that SSAA completes its execution faster than that of the proposed algorithm. However, the revenue obtained by SSAA is lower than that of the proposed algorithm (see Fig. 5.5). Moreover, CAA takes more time to complete its execution and has a higher rate of growth. Additionally, we did not consider the execution time of the optimal solution because it has a significantly higher execution time.

Prototype Model: We use a Workstation (WS) as the MBS, a UAV with a Raspberry Pi, and two mobile phones with pulse oximeter and ECG sensors as WBANs, as shown in Fig. 5.9. Moreover, the specification of each device in the prototype setup is given in Table 5.4. WS, mobile phones, and UAV are connected using 4G mobile hotspot connection. Pulse oximeter and ECG sensor collect physiological data from the patient and send it to mobile phone. Then, the UAV collects physiological data from the phones and performs FL training with the help of WS.

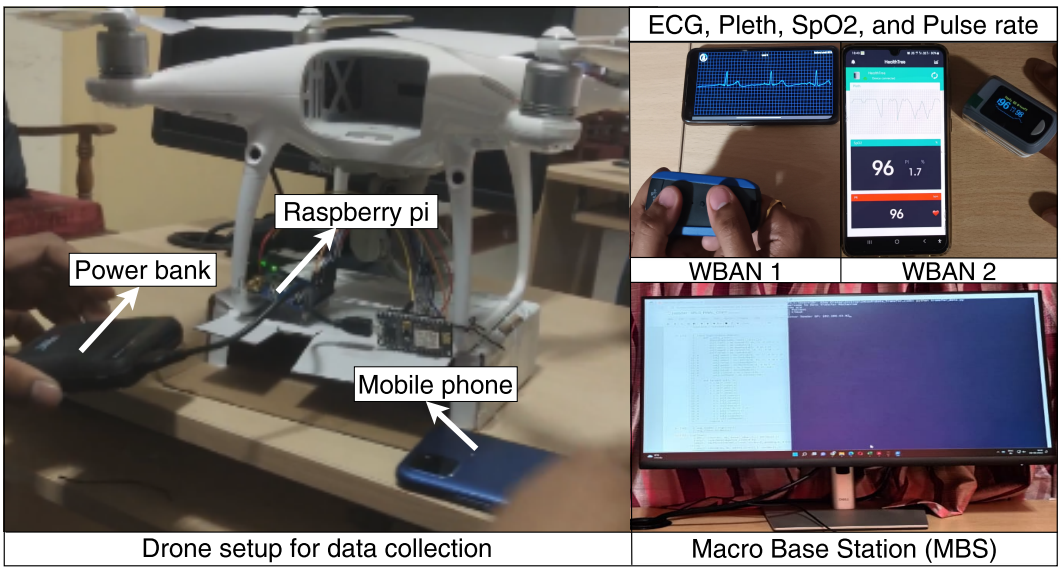

Fig. 5.9. Prototype setup.

Fig. 5.8b compares the performance of the proposed model on physiological data sizes ranging from 0.33 MB to 2.35 MB. The results show that the revenue obtained in the simulation is higher than that of the prototype implementation due to differences

Table 5.4: Device specifications

Devices	Specification
Raspberry Pi	**Model:** Raspberry Pi 4 Model B, **SOC:** Broadcom BCM2711, Cortex-A72 (ARM-v8) 64-bit SoC, **CPU:** 1.5 GHz 64-bit quad-core ARM Cortex- A72 CPU, **RAM:** 8GB LPDDR4 SDRAM, **WiFi:** Dual-band 802.11 b/g/n/ac wireless LAN
Workstation	**Model:** Dell Precision 3640 Workstation, **Processor:** 11th generation Core-i7-10700 CPU (8 Core(s)) @4.10 GHz, **RAM:** 32 GB
UAV	**Model:** Phantom 4 Pro V2.0, 5 direction obstacle sensing, 1 inch 20 MP CMOS sensor
ECG sensor	**Model:** SanketLife Pro-Plus ECG sensor, 12-Lead ECG Monitor, **Weight:** 120 gms,
Pulse sensor	**Model:** Pulse Oximeter, **Operating Environment:** $+10^0C \sim +40^0C$, **Measurements:** SpO2, Pulse rate, Pleth
Mobile	**Model:** Samsung Galaxy A22 5G, Oneplus Nord CE 5G **RAM:** 8 GB, 8 GB & **Memory** 128 GB, 128 GB **Android Version:** 13, 12

in communication technologies. The prototype uses a 4G mobile hotspot to transmit physiological data from mobile devices to UAV, whereas the simulation assumes 5G communication. Since 4G technology offers lower data transmission speeds and efficiency compared to 5G, this results in longer transmission times and higher energy consumption in the prototype, ultimately leading to reduced performance. Moreover, the devices used in the prototype model are not the same configured devices as those considered in the simulation, which led to higher computation times and energy costs, ultimately resulting in lower utility and further contributing to the performance differences. We also observe that the curves for both implementations show similar results, indicating the applicability of the proposed model in real-world scenarios.

5.6 Summary

This chapter proposed a UAV-assisted WBAN-based FL framework underlying 5G network, where UAVs collected physiological data from WBANs and performed FL training. Formulated an optimization problem by maximizing the revenues of both WBANs

and UAVs for providing physiological data and computational resources, respectively, via RA, as an NP-hard problem. Further, a matching and graph coloring-based efficient RA algorithm was applied to maximize the overall revenue, considering the minimum and the maximum PRB demand of WBANs. Extensive simulations and prototype results on real-world data demonstrated the effectiveness of the proposed model, achieving an average revenue of 92.8% of the optimal value compared to that of 86.6% and 76.6% for SSAA and CAA, respectively. Although UAVs can assist resource-constrained LDs in WBANs, they also introduce privacy vulnerabilities, as the data transmission process may be susceptible to unauthorized access or breaches. Therefore, the next chapter addresses these privacy concerns by integrating privacy-preserving techniques, such as DP and HE.